Comparison of mechanical properties, marginal adaptation and surface roughness of 3D printed provisional crown by printing angle

Choi, Eunah

Department of Industrial Dentistry

Graduate School

Yonsei University

Comparison of mechanical properties, marginal adaptation and surface roughness of 3D printed provisional crown by printing angle

Advisor Jung, Bock-Young

A Master's Thesis Submitted
to the Department of Industrial Dentistry
and the Committee on Graduate School
of Yonsei University in Partial Fulfillment of the
Requirements for the Degree of
Master of Science in Dentistry

Choi, Eunah

June 2025

Comparison of mechanical properties, marginal adaptation and surface roughness of 3D printed provisional crown by printing angle

This Certifies that the Master's Thesis of Choi, Eunah is Approved

Committee Chair	**Kim, Kee-Deog**
Committee Member	**Jung, Bock-Young**
Committee Member	**Doh, Re-Mee**

Department of Industrial Dentistry
Graduate School
Yonsei University
June 2025

TABLE OF CONTENTS

LIST OF FIGURES

LIST OF TABLES

ABSTRACT

Comparison of mechanical properties, marginal adaptation and surface roughness of 3D printed provisional crown by printing angle

As dental procedures increasingly adopt digital workflows, provisional prostheses are now being fabricated using three-dimensional (3D) printing. Among the different types of 3D printers, LCD 3D printers have recently begun to appear in clinical use due to their low cost and acceptable performance. However, the mechanical and surface properties of printed objects can be influenced by the printing angle. This study aimed to evaluate the influence of various printing angles on the fracture strength, marginal adaptation, and surface roughness of a single provisional crown fabricated using an LCD 3D printer.

The master model was prepared by clinically preparing a phantom tooth and duplicating it in cobalt-chromium. Two types of specimens, a provisional crown and a disc, were designed. Each was printed at four angles (0°, 15°, 30°, and 45°) using a urethane dimethacrylate (UDMA) based resin. A total of 76 specimens were fabricated, with 19 for each angle in each test.

A universal testing machine was employed for fracture testing. The crosshead was set to move at a speed of 1 mm/min during load application. Marginal adaptation was evaluated through the silicone replica technique (SRT), with measurements taken at the buccal, mesial, distal, and lingual surfaces. Surface roughness was measured at nine points on each disc using a confocal laser scanning microscope. The average of these values was used for each specimen, and group means and standard deviations were compared by angle. The Shapiro–Wilk test was first conducted to assess normality.

When normality was satisfied, one-way ANOVA was applied. In cases where this assumption was not fulfilled, the Kruskal–Wallis test was performed instead. Bonferroni post-hoc comparisons were carried out following the primary tests to assess differences between individual groups.

The analysis revealed statistically significant differences according to the printing angle in all three test parameters ($p < 0.05$). Specimens printed at 0° and 15° exhibited higher fracture strength compared to those printed at 30° and 45°, and all groups exceeded the average maximum occlusal force. The smallest mean and standard deviation of marginal gap were observed in the 30° group, and all groups met the clinically acceptable threshold of less than 120 μm. Surface roughness increased in the order of 0°, 45°, 30°, and 15°. Except for the 0° group, higher printing angles resulted in narrower stair-step spacing and lower surface roughness.

The conclusion of this study is that the printing angle affects the properties of objects fabricated using an LCD printer. However, no single angle demonstrated superiority in all aspects. Therefore, the printing angle should be selected based on specific clinical situations. Based on the results of this study, the use of 0° and 30° printing angles can be recommended.

Key words : 3D printer, LCD 3D printer, printing angle, fracture strength (FS), marginal adaptation, silicone replica technique (SRT), surface roughness

1. INTRODUCTION

With the progressive adoption of digital technologies in the dental field, an increasing number of clinical procedures are conducted within a digital workflow. Dental professionals acquire patient data through pre- and post-treatment scans to develop precise treatment plans, which guide the corresponding procedures. These datasets are subsequently used to fabricate various dental prostheses and devices, including diagnostic models, custom trays, surgical guides, provisional fixed dental prosthesis (FDP), definitive FDP, and orthodontic appliances (Kessler et al., 2019).

Provisional FDPs play a key role in protecting the dentin and pulp from external exposure until the definitive FDP is placed. They also contribute to occlusal stability, maintenance of adjacent tooth position, preservation of periodontal health and esthetics, and support for diagnostic procedures prior to final prosthesis placement (Hasanzade et al., 2023). To fulfill these functions, provisional FDPs must possess sufficient mechanical strength to withstand occlusal forces, exhibit excellent marginal adaptation, and have a smooth surface that minimizes bacterial proliferation (Alharbi & Osman, 2021). Inadequate marginal adaptation may lead to cement washout and subsequent plaque accumulation, potentially resulting in periodontal complications or esthetic issues (Park et al., 2019).

Three-dimensional (3D) printing technology is increasingly being applied to the fabrication of provisional FDPs. The primary clinical advantages of 3D printing include rapid production and the ability to reprint the prosthesis using the original digital file in the event of damage prior to final placement (Yildirim et al., 2024). In addition, compared to subtractive manufacturing, 3D printing uses only the amount of material required for fabrication, thereby reducing material waste and minimizing the use of consumables such as milling burs (Alharbi et al., 2016).

Among the various 3D printing techniques, photopolymerization-based methods such as stereolithography (SLA) and digital light processing (DLP) are the most commonly used in dentistry (Reymus et al., 2020). These two methods differ in terms of light source and system configuration. SLA printers use a UV laser as the light source, and the laser beam is selectively reflected across the x- and y-axes by galvo mirrors to cure the resin point by point (Caussin et al., 2024; Tsolakis et al., 2022). In contrast, DLP printers employ an LED light source, and a digital micromirror device (DMD) reflects light to cure one layer at a time in its entirety (Tsolakis et al., 2022).

Recently, liquid crystal display (LCD) printers, which utilize a photopolymerization mechanism similar to SLA and DLP, have been introduced into the dental field. LCD printers employ densely arranged monochromatic LED light sources in a chip-on-board (COB) configuration. The emitted light is collimated through COB and Fresnel lenses before passing through an LCD panel (Shafique et al., 2024). The LCD panel masks regions that are not to be printed (Caussin et al., 2024).

LCD printers have several structural and functional advantages and disadvantages compared to conventional SLA and DLP systems. Because the light in LCD printers is projected in a nearly vertical and collimated manner, the pixel distortion that can occur in DLP systems is reduced (Tsolakis et al., 2022). Unlike SLA, which cures the resin point by point, LCD printers cure the resin layer by layer, resulting in a relatively faster printing speed similar to that of DLP systems (Tsolakis et al., 2022). In terms of resolution, LCD printers theoretically offer higher resolution than DLP printers due to a greater number of pixels; however, due to the structure of the LCD printer, optical convergence between adjacent pixels may occur, reducing the actual resolution compared to the theoretical value (Caussin et al., 2024; Shafique et al., 2024). Furthermore, the crossed polarizer configuration of the LCD panel causes significant ultraviolet light loss, which may lead to lower irradiance levels than those of DLP systems (Shafique et al., 2024). However, LCD printers are relatively inexpensive compared to SLA and DLP systems because the cost of optical components

is lower (Tsolakis et al., 2022). This cost-effectiveness has contributed to their increasing popularity, especially in contexts where budget constraints are significant.

Based on these structural characteristics and functional advantages and disadvantages, comparative studies have reported that specimens printed with LCD printers demonstrated lower strength than those produced with DLP printers, although the values were considered clinically acceptable (Chen et al., 2021). Specimens fabricated using LCD printers also exhibited more uniform and smoother surfaces compared to those produced with DLP printers (Wada et al., 2022). Although SLA systems have been reported to provide higher dimensional accuracy than DLP and LCD systems due to differences in printing mechanisms, studies specifically evaluating the dimensional accuracy of LCD printers remain limited (Caussin et al., 2024).

According to previous studies, the results of 3D printing can vary depending on several parameters, including the type of material used, printer resolution, light intensity, printing speed, post-curing time, and printing angle (Grymak et al., 2021).

Dedicated liquid resins are used as materials for 3D printing, typically consisting of photopolymerizable oligomers, reactive diluents, photoinitiators, and various additives (Yang et al., 2024). Among these components, the chemical structure of the monomers forming the oligomers and the overall resin composition directly affect the mechanical properties and dimensional accuracy of the printed objects (Yang et al., 2024). Therefore, the selection of monomers is a critical factor. The most commonly used monomers are urethane dimethacrylate (UDMA) and bisphenol A-glycidyl methacrylate (Bis-GMA) (Lin et al., 2020). UDMA, in particular, contains flexible urethane linkages and an aliphatic core, resulting in lower viscosity than Bis-GMA and a smaller molecular size, which contributes to a higher double bond concentration (Kessler et al., 2019). Accordingly, its maximum polymerization rate has been reported to be approximately three times faster (Lin et al., 2020). These structural features contribute to the formation of chemically and physically stable polymers with high mechanical strength (Rosentritt et al., 2021). However, both UDMA and Bis-

GMA are dimethacrylate-based monomers with high viscosity, which limits their flowability during the printing process; therefore, reactive diluents must be incorporated (Lin et al., 2020).

As such, various factors, including printer type, material composition, and processing conditions, affect the outcomes of 3D printing. In particular, among the processing conditions, the printing angle has been reported as a key variable that directly influences mechanical properties, dimensional accuracy, and surface characteristics (Grymak et al., 2021).

Numerous studies have investigated the effect of printing angle on printing outcomes using provisional FDP resins with SLA and DLP printers. In studies using SLA printers, fracture strength was compared, and higher values were observed at 0°, 30°, and 150°, while significantly lower values were reported at 90° (Diken Turksayar et al., 2022). In studies using DLP printers, flexural strength was evaluated, with results varying depending on the specimen type. One study employing bridge-shaped specimens reported the highest flexural strength at 30° and the lowest at 90° (Sang-Mo et al., 2019). In contrast, another study using bar-shaped specimens found the highest flexural strength at 90° (Fábio Hideo et al., 2025). In addition, a study that assessed marginal and internal adaptation using a DLP printer recommended 0° and 30° as the most optimal printing angles (Ryu et al., 2020). In a comparative study including all three types of photopolymerization-based printers, 0° and ± 30° were reported to yield the best results in terms of trueness, marginal adaptation, and internal adaptation (Alghauli et al., 2025). A surface roughness study using an SLA printer found that the lowest surface roughness was observed at 0° before polishing, while the highest was reported at 90° (Alharbi & Osman, 2021).

In previous studies on printing angle for provisional FDPs, various angles such as 0°, 30°, 45°, 60°, and 90° were investigated using different types of 3D printers and materials with various compositions.

Most existing studies have focused on either single-method approaches using subtractive manufacturing or additive manufacturing, such as SLA or DLP printing, or on comparative studies based on various manufacturing methods. In contrast, LCD printers were originally developed for non-dental applications and have only recently been introduced into the dental field. As a result, studies investigating the effect of printing angle using LCD printers remain insufficient.

Therefore, the purpose of this study was to fabricate single-unit provisional crowns using an LCD 3D printer and to evaluate the effect of different printing angles on fracture strength, marginal adaptation, and surface roughness. The null hypothesis of this study was that there would be no significant differences in fracture strength (FS), marginal adaptation, or surface roughness of single provisional FDPs fabricated using an LCD printer depending on the printing angle.

2. MATERIALS AND METHODS

2.1. Test specimens and materials

To fabricate provisional crown specimens, the maxillary second molar of a dental phantom tooth (PR01; OSSTEM IMPLANT, Seoul, Korea) was positioned to a base block to produce a model. The phantom tooth was prepared with an occlusal reduction of 2.0 mm and an axial reduction of 1.5 mm using a deep chamfer margin (Doh et al., 2025).

A prepared tooth model was scanned using an intraoral scanner (TRIOS 5; 3Shape A/S, Copenhagen, Denmark), and the acquired data was used to replicate a cobalt-chromium model (AM01; Attometal, Gimpo, Korea) using a metal 3D printer (David 1.0; MERAIN, Incheon, Korea) employing selective laser sintering (Diken Turksayar et al., 2022).

Since the surface of the replicated metal model was glossy, a thin layer of scan spray (EASYSCAN; PD Dental, Seoul, Korea) was applied to enhance scanning accuracy. The replica model was then rescanned and exported as an STL file using dental design software (3Shape; Copenhagen, Denmark). A test specimen of a single provisional FDP was designed with a cement gap of 0.05 mm, a marginal offset of 0.8 mm above the finish line and an occlusal thickness of 2.0 mm (Figure 1). These crown specimens were used for the test of FS and marginal adaptation.

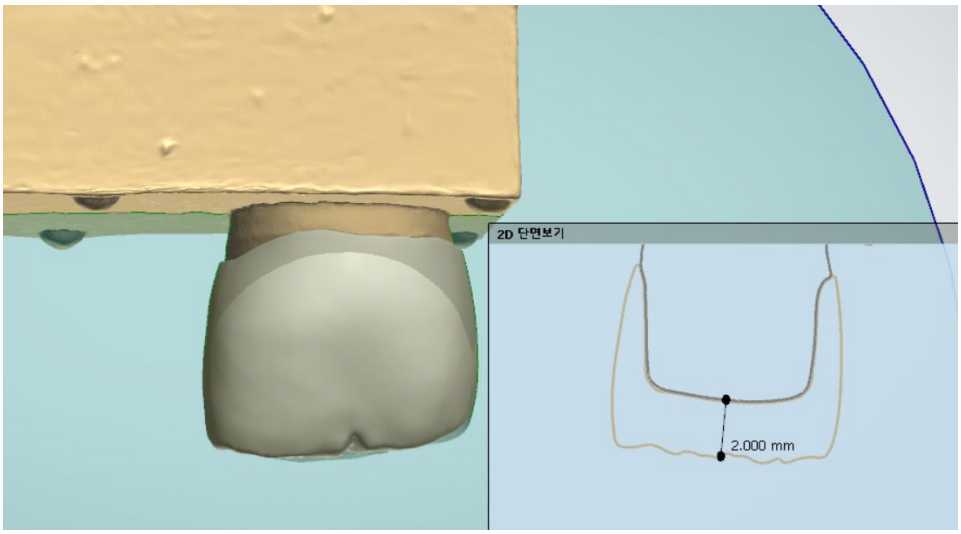

Figure 1. Occlusal thickness of provisional crown specimen.

For surface roughness testing, circular disc specimens with a diameter of 5 mm and a thickness of 2 mm were designed using CAD software (Netfabb; Autodesk Inc, San Rafael, USA) (Doh et al., 2025). Both single FDP crowns and disc specimens were printed at four angles: 0°, 15°, 30° and 45°. For crown specimens, the 0° angle was defined as placing the occlusal surface parallel to the build platform (Diken Turksayar et al., 2022). For disc specimens, the 0° angle was defined as placing the largest circular surface parallel to the platform (Figure 2). Each specimen was positioned at the intended angle using slicing software (Anycubic Photon Workshop; Anycubic, Shenzhen, China).

All test specimens were printed using an LCD 3D printer (Photon Mono M7 Pro; Anycubic, Shenzhen, China) with a UDMA-based 3D printing resin (OneJet C&B; OSSTEM IMPLANT, Seoul, Korea) (Figure 3, Table 1).

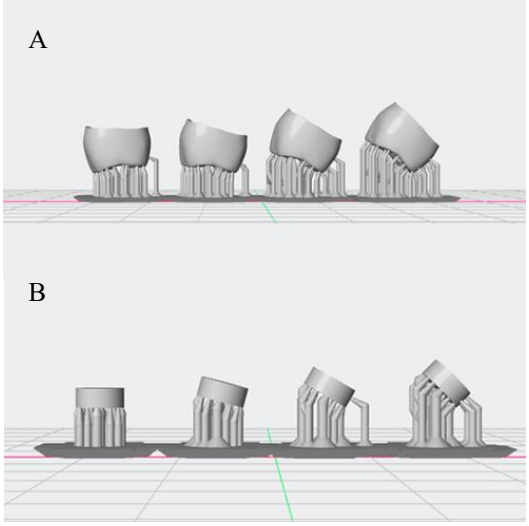

Figure 2. Provisional crowns and discs were printed at 4 printing angles (0°, 15°, 30°, 45°) using a 3D printer. (A) Crown specimen, (B) Disc specimen

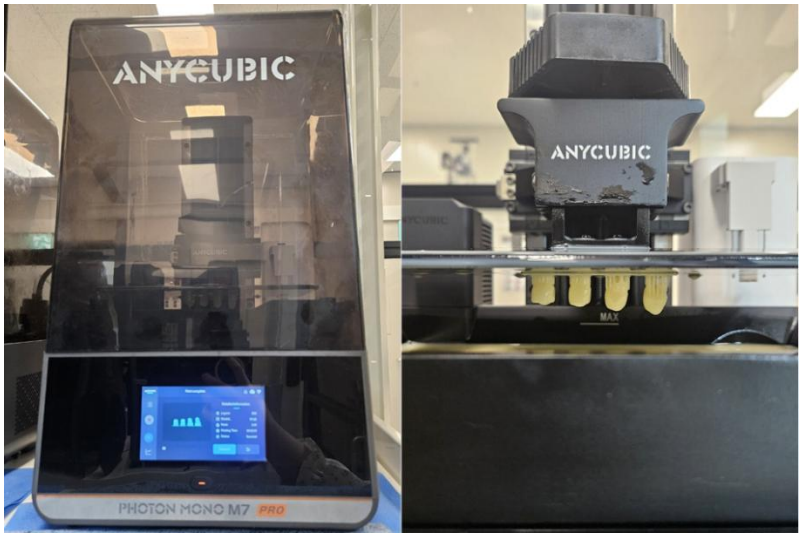

Figure 3. LCD 3D printer (Photon Mono M7 Pro; Anycubic, Shenzhen, China).

After the printing process, the supports structures were removed in accordance with the manufacturer's guidelines. Printed objects were cleaned in an ultrasonic cleaner (Powersonic 520; Hwashin Tech, Seoul, Korea) filled with isopropyl alcohol (IPA 99.9%; Ecochem, Korea) for 3 minutes. If uncured resin remained, an additional 3-minute cleaning was performed under the same conditions. Post-curing was carried out for 7 minutes using a light-curing unit (OneCure Plus; OSSTEM IMPLANT, Seoul, Korea).

For FS test preparation, temporary cement (Temp Bond NE; Kerr Dental, Brea, CA, USA) was mixed for approximately thirty seconds and applied to the internal surface of the provisional crown specimens, which were then seated onto cobalt-chromium dies. A static load of fifty newtons was applied using a metal weight for seven minutes to ensure proper adhesion. After setting of the cement, excess material was removed using a dental explorer (Reeponmaha et al., 2020).

The specimens were divided into four groups based on the printing angle (0°, 15°, 30°, and 45°) for comparison. Each group consisted of 19 specimens for each test. The sample size was determined using a power analysis based on an effect size of 0.4, a power of 80%, and a significance level of 5%. The analysis was performed using G*Power software (version 3.1.9.2; Heinrich Heine University Düsseldorf).

A single researcher performed all tests and curated the data to minimize variability across the experimental process.

Table 1. Specifications of devices.

	Type	Information	Manufacturer
Anycubic Photon Mono M7 Pro	3D printer	Liquid crystal display (LCD) Build volume (mm): 223×126×230 Layer height (mm): ≥0.01 LCD Resolution: 13,320×5,120 pixels XY axis pixel: 16.8×24.8 μm	Anycubic, Shenzhen, China
OneJet C&B	Printing material	Polymer: UDMA Layer thickness: 50 μm Flexural strength: 121 MPa Dimensional accuracy: 213 μm	OSSTEM IMPLANT, Seoul, Korea

2.2. Fracture strength

FS was measured with a universal testing machine (Instron 3365; Instron Corporation, USA) with a load cell rated at 5 kN and the crosshead speed was set to 1 mm/min. A metal rod with a diameter of 3.0 mm was positioned to apply axial force at the central fossa of the crown and the load was continuously applied until the specimen fractured (Figure 4). The maximum load at fracture was recorded in newton (N).

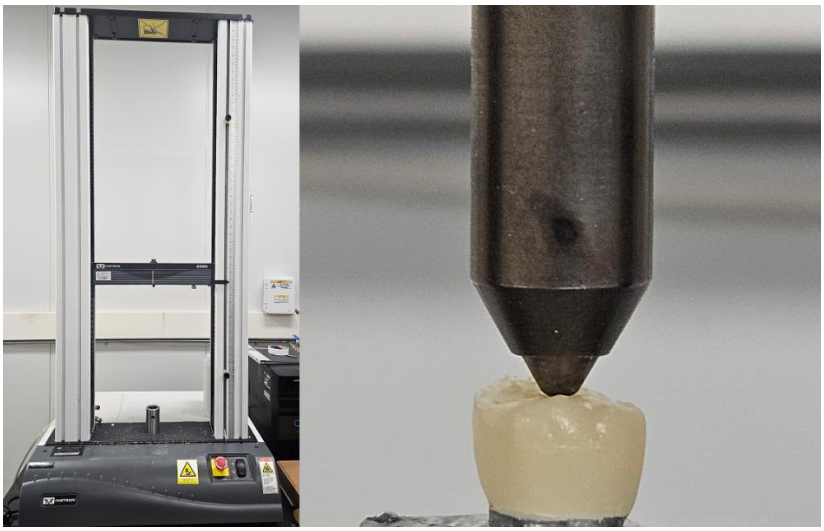

Figure 4. A universal testing machine (Instron 3365; Instron Corporation, USA).

2.3. Marginal adaptation assessment

The marginal adaptation of the crowns was evaluated using the silicone replica technique (SRT) (Cho et al., 2023; Ryu et al., 2020; Son et al., 2019). Silicone impression materials were used, including a light body (HySil LIGHT PLUS; OSSTEM IMPLANT, Seoul, Korea), a regular body (HySil MONO PLUS; OSSTEM IMPLANT, Seoul, Korea), and a putty (HySil PUTTY; OSSTEM IMPLANT, Seoul, Korea).

Light body silicone was injected into the intaglio surface of the crown specimen using a 1:1 cartridge-type dispensing gun with an automixing tip. The crown was then seated onto the cobalt-chromium die and compressed under a constant load of 50 N using a metal weight. After the light body had hardened, the crown was gently removed with the set light body attached.

Next, the internal space of the crown was filled with regular body silicone, and the putty silicone impression material was loaded into a custom mold prepared for this procedure. The mold and crown were joined and fixed in position using a custom jig to ensure consistent alignment. After complete setting of the silicones, the crown, jig, and mold were separated (Figure 5).

The silicone replica was sectioned using a cutting template that matched the mold design and featured a cross-shaped guide with a thickness of 0.5 mm (Son et al., 2019). Sectioning was performed in both buccolingual and mesiodistal directions (Figure 6A). The thickness of the light body silicone at the buccal, mesial, distal and lingual margins was measured under a digital stereo microscope (VHX-1000; Keyence, Osaka, Japan) at ×100 magnification (Figures 6B, 7). The average of the four measured values was recorded as the final marginal gap for each specimen (Ryu et al., 2020).

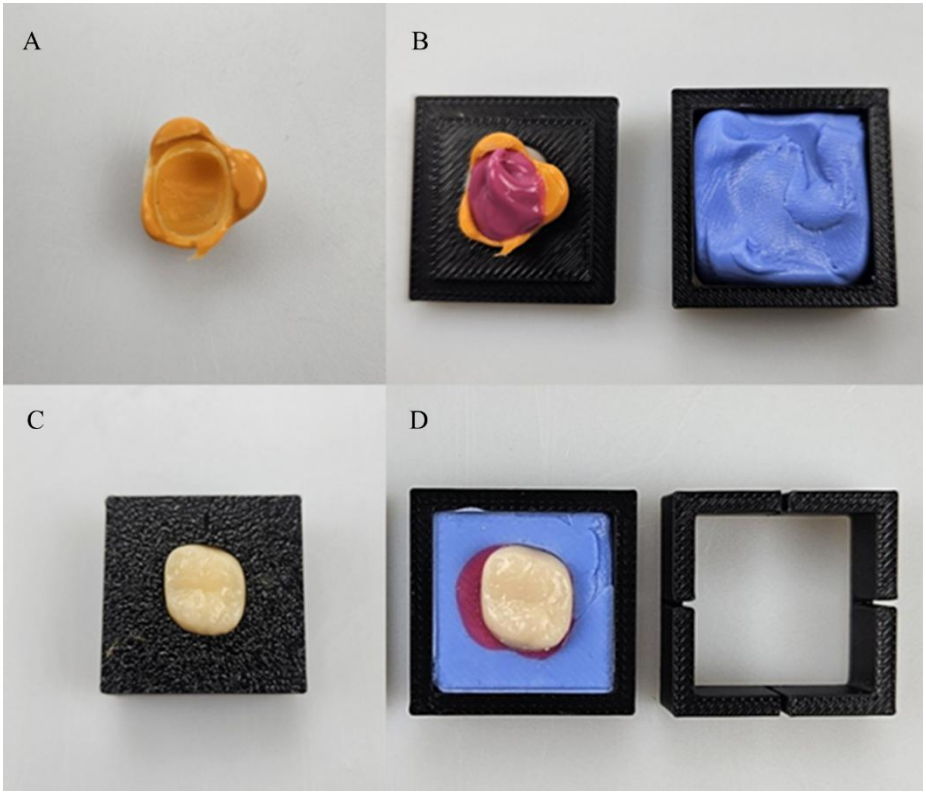

Figure 5. Procedures of the silicone replica technique for marginal adaptation.

(A) Registration of the gap between the die and the crown using light body silicone.

(B) Regular body silicone filling of the crown, and putty embedding using a custom mold.

(C) The mold and crown were aligned and fixed using a custom jig.

(D) The crown, jig, and mold were separated, and the cutting template was placed.

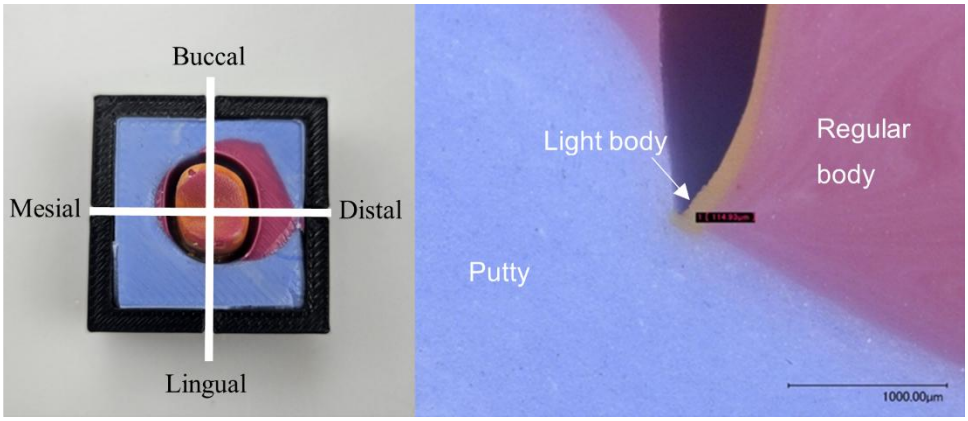

Figure 6. Sectioning and marginal gap measurement of the silicone replica using a cutting template.

(A) The cutting template to divide the specimen into buccal–lingual and mesial–distal sections.

(B) Measurement points for the marginal gap.

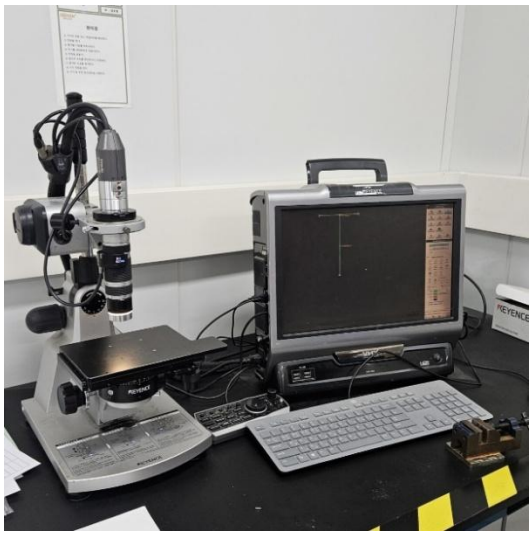

Figure 7. A digital stereo microscope (VHX-1000; Keyence, Osaka, Japan).

2.4. Surface roughness

The arithmetic average roughness, abbreviated as Ra and the ten-point average roughness, abbreviated as Rz were measured for each specimen.

Surface roughness was evaluated with a confocal laser scanning microscope (CLSM) (OLS5000-EAF; OLYMPUS, Japan), with features a vertical resolution of 0.5 nm and a repeatability of 0.012 μm (Figure 8). For each specimen, one central location and two marginal locations were selected (Murat et al., 2019). Three measurements were taken at each location resulting in a total of nine values per specimen. To ensure consistency in surface roughness measurement, the step-shaped layers formed during the additive printing process were aligned horizontally before scanning. The average of these values was used to represent the surface roughness of each specimen (Doh et al., 2025; Murat et al., 2019).

The objective magnification was set to 50×, the zoom factor to 1×, and the scan field size was 259×1192 μm².

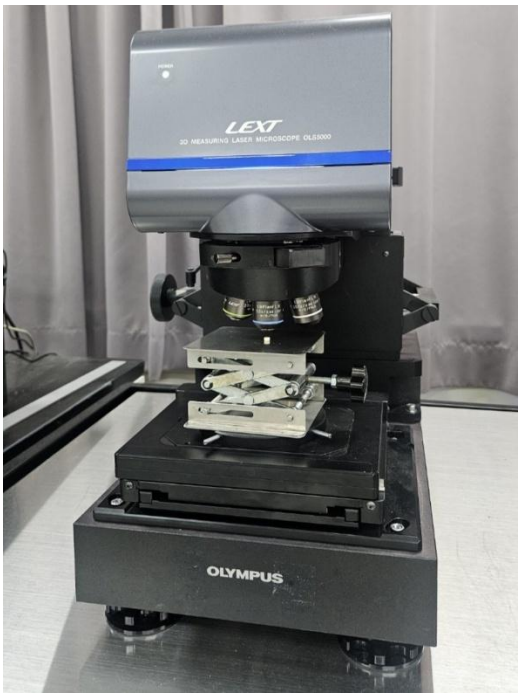

Figure 8. Confocal Laser Scanning Microscope (OLS5000-EAF; OLYMPUS, Japan).

2.5. Statistical analysis

Statistical analysis was carried out using SAS software version 9.4 (SAS Institute Inc., Cary, NC, USA). Normality within each group was evaluated with the Shapiro–Wilk test. One-way ANOVA was applied when all groups showed normal distribution; otherwise, the Kruskal–Wallis test was used. Depending on the type of outcome variable, post hoc comparisons were conducted using the Bonferroni method. Statistical significance was defined as $p < 0.05$.

3. RESULT

3.1. Fracture strength

The mean FS of the provisional crowns was assessed based on the printing angle. The group printed at 15° showed the highest mean strength of 2,220.43 ± 392.97 N, followed by the 0° group with 2,195.99 ± 414.58 N. In contrast, the 30° group showed the lowest value of 1,782.51 ± 111.77 N, and the 45° group exhibited a slightly higher strength of 1,847.41 ± 135.73 N (Table 2, Figure 9).

The Kruskal–Wallis test revealed a significant difference among the groups ($p < 0.05$). Therefore, post hoc analysis was performed to determine the differences between the groups. The 30° and 45° groups exhibited significantly lower FS compared to the 0° and 15° groups. Although no significant differences were observed between the 0° and 15° groups or between the 30° and 45° groups, notable distinctions were identified in the other comparisons.

Table 2. Comparison of fracture strength.

Printing angle	Fracture strength (N)						
	Mean	**SD**	**Median**	**IQR**	**Minimum**	**Maximum**	***p*-value***
0° [a]	2195.99	±414.58	2070.41	607.67	1639.64	2929.65	<.0001
15° [a]	2220.43	±392.97	2079.18	797.52	1764.45	2777.57	
30° [b]	1782.51	±111.77	1795.98	179.36	1524.65	1970.56	
45° [b]	1847.41	±135.73	1831.97	180.14	1628.12	2125.78	

SD=standard deviation, IQR=Inter Quartile Range

*The *p*-value was obtained from the Kruskal-Wallis test. The difference alphabet means a significant difference between the printing angle groups for Bonferroni's post-hoc analysis.

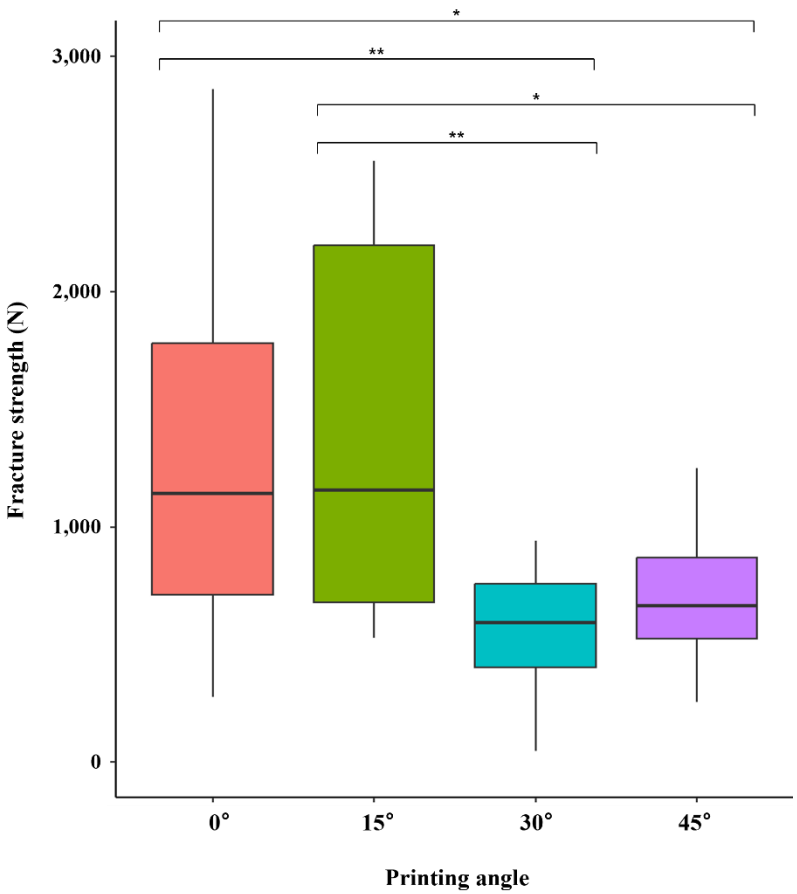

Figure 9. Fracture strength according to printing angle.

*p-value < 0.05; **p-value < 0.01; ***p-value < 0.001; Statistically significant differences were found in pairwise comparisons across groups, based on Bonferroni's post-hoc analysis.

3.2. Marginal adaptation assessment

The marginal adaptation of the provisional crowns was evaluated by calculating the mean distance measured at the buccal, mesial, distal and lingual surfaces. The group printed at 30° showed the smallest average marginal gap, 97.88 ± 8.49 μm, followed by the 45° group with 107.46 ± 28.57 μm. The 0° and 15° groups showed the largest values, with 116.60 ± 13.80 μm and 116.34 ± 19.15 μm, respectively (Table 3, Figure 10).

One-way ANOVA revealed statistically significant differences among the groups ($p < 0.05$). Post hoc analysis indicated that the 30° group exhibited significantly smaller marginal gap values compared to the 0° and 15° groups. Significant differences were identified only between the 30° and 0° groups and between the 30° and 15° groups. These results suggest that printing at a 30° angle may enhance the marginal adaptation of 3D printed provisional crowns.

Table 3. Comparison of marginal adaptation.

Printing angle	Marginal adaptation (μm)						
	Mean	SD	Median	IQR	Minimum	Maximum	*p*-value*
0° [a]	116.60	±13.80	117.50	19.83	88.14	138.26	0.0091
15° [a]	116.34	±19.15	114.97	26.69	76.46	148.94	
30° [b]	97.88	±8.49	96.67	16.27	84.71	113.35	
45° [ab]	107.46	±28.57	113.52	51.18	49.14	148.82	

SD=standard deviation, IQR=Inter Quartile Range

*The *p*-value was obtained from the one-way ANOVA (analysis of variance) test. The difference alphabet means a significant difference between the printing angle groups for Bonferroni's post-hoc analysis.

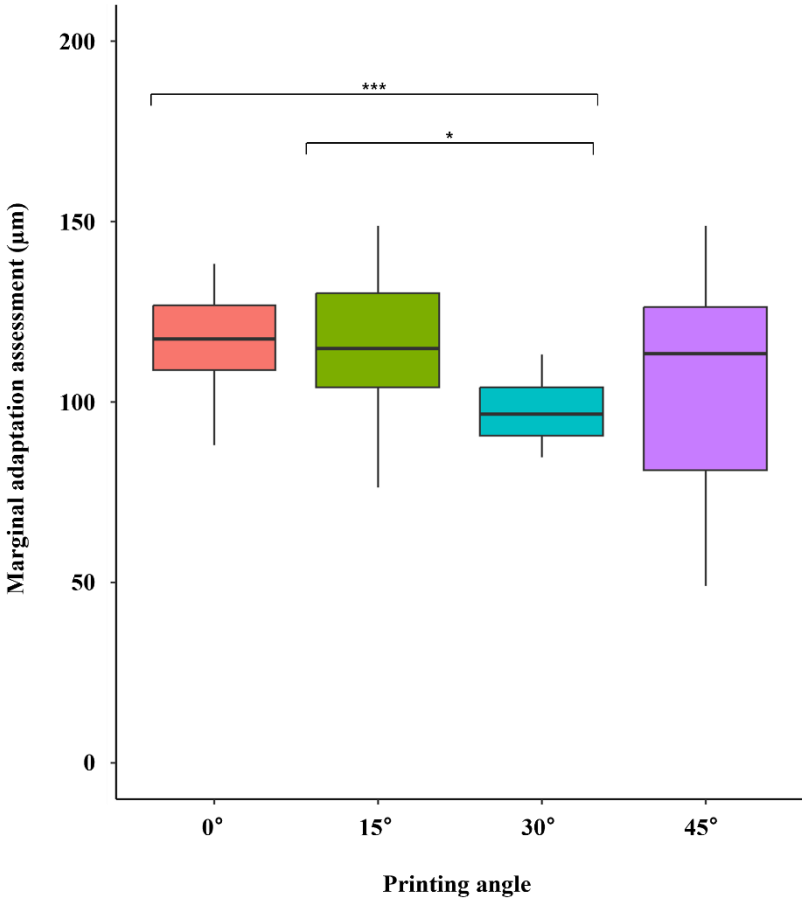

Figure 10. Marginal adaptation according to printing angle.

*p-value < 0.05; **p-value < 0.01; ***p-value < 0.001; Statistically significant differences were found in pairwise comparisons across groups, based on Bonferroni's post-hoc analysis.

3.3. Surface roughness

The surface roughness values were assessed using Ra and Rz (Figure 11). The surface roughness varied depending on the printing angle. The Kruskal–Wallis test revealed statistically significant differences in both Ra and Rz values ($p < 0.05$). Therefore, post hoc analysis was conducted to identify specific trends.

For Ra, a clear increasing trend was found in the order of 0°, 45°, 30°, and 15°. The 0° group showed the smoothest surface with a mean Ra of 1.10 ± 0.16 μm, whereas the 15° group had the roughest surface at 4.39 ± 0.15 μm. In the case of Rz, a statistically significant difference was confirmed that increased in the order of 0°, 45°, 30°, and 15°, as with Ra. The 0° group recorded the lowest Rz value of 6.98 ± 1.84 μm, while the 15° group showed the highest at 21.45 ± 1.57 μm (Table 4, Figure 12). These findings indicate that printing angles have a significant influence on both the average and peak-to-valley surface roughness. Overall, the results suggest that printing at 0° yields a smoother and more uniform surface, providing the highest surface quality.

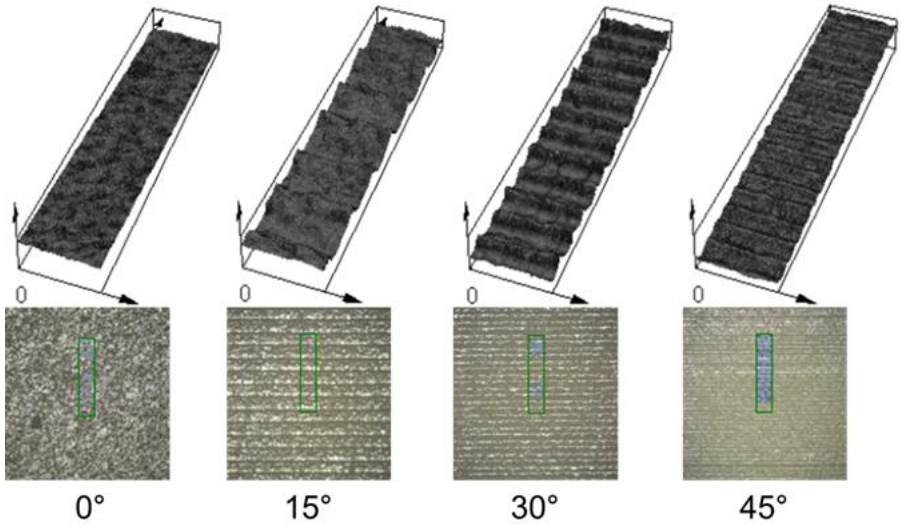

Figure 11. Surface roughness images according to printing angle.

Table 4. Comparison of surface roughness.

Printing angle	Ra(μm)			Rz(μm)		
	Mean±SD	**Median(IQR)**	***p*-value***	**Mean±SD**	**Median(IQR)**	***p*-value***
0°	1.10±0.16	1.04(0.21) [a]	<.0001	6.98±1.84	6.36(2.60) [a]	<.0001
15°	4.39±0.15	4.44(0.29) [b]		21.45±1.57	21.33(1.65) [b]	
30°	3.90±0.48	3.77(0.23) [c]		19.75±4.82	17.63(2.83) [c]	
45°	2.79±0.16	2.75(0.28) [d]		14.50±1.94	15.00(3.02) [d]	

SD=standard deviation, IQR=Inter Quartile Range

*The *p*-value was obtained from the Kruskal-Wallis test. The difference alphabet means a significant difference between the printing angle groups for Bonferroni's post-hoc analysis.

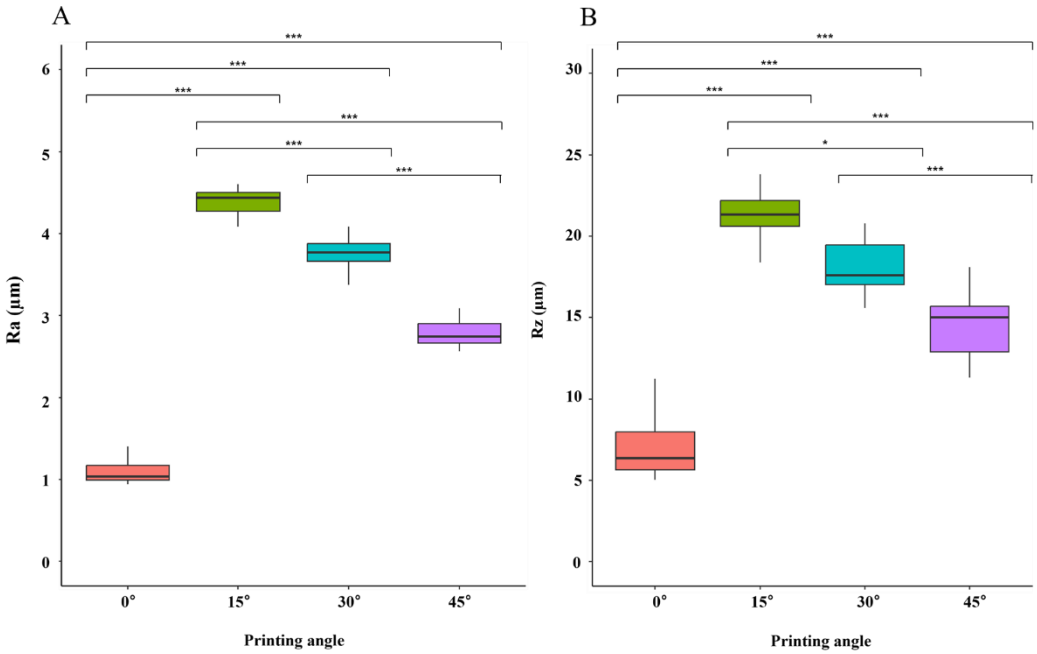

Figure 12. Surface roughness (Ra, Rz) according to printing angle.

(A) Ra of Surface roughness, (B) Rz of Surface roughness

*p-value < 0.05; **p-value < 0.01; ***p-value < 0.001; Statistically significant differences were found in pairwise comparisons across groups, based on Bonferroni's post-hoc analysis.

4. DISCUSSION

The printing angle, which served as the independent parameter in this study, showed a statistically significant influence on FS, marginal adaptation, and surface roughness. Based on these results, the null hypothesis, which stated that there would be no statistically significant differences among groups, was rejected.

FS exhibited significantly higher values in the 0° and 15° groups compared to the 30° and 45° groups. This trend may be explained by the improved overall mechanical strength when the direction of occlusal loading during printing is perpendicular to the printed layers.

This finding aligns with a previous study reporting that the highest fracture strength (FS) was observed in provisional FDPs printed at 0° (Diken Turksayar et al., 2022). These results can be explained by the orientation of the printed layers: when the printing direction was perpendicular (vertical) to the loading direction—as in the 0° orientation used in the present study—there was less layer delamination. In contrast, when the printing orientation was horizontal (90°), the layers were parallel to the loading direction, promoting separation between layers and resulting in lower compressive strength (Alharbi et al., 2016).

Masticatory force varies significantly between individuals, therefore, provisional FDP should possess sufficient mechanical strength, even for short-term use. Adult males can exert up to 909 N of occlusal force in the molar region (Reymus et al., 2020). In this study, even the lowest group, printed at 30°, showed a mean FS exceeding 1500 N, which far surpasses the maximum occlusal force in adult males. Therefore, all tested groups of 4 printing angles could provide clinically acceptable mechanical strength. In particular, the printing angles of 0° and 15° may serve as reliable

options for fabricating provisional crowns owing to its superior performance for the patients with strong occlusal forces or bruxism (Diken Turksayar et al., 2022).

These findings may also be attributed to the material properties used in this study. Due to its urethane linkages and aliphatic structure, UDMA exhibits high mechanical strength and low polymerization shrinkage after curing, while showing a rigid backbone (Kessler et al., 2019; Rosentritt et al., 2021). As a result, sufficient strength was maintained across all groups regardless of the printing angle.

The marginal gap according to the printing angle was significantly smaller in the 30° group than in the 0° and 15° groups. Ryu et al. (2020) reported that provisional crowns fabricated at various printing angles using a DLP printer. The 150° group (equivalent to 30° in the present study) showed the smallest marginal gap. which was explained due to differences in the shape of each layer and the degree of polymerization shrinkage depending on the printing angle. These results suggest that the layer relationship along the crown margin may be more stable and the degree of polymerization shrinkage is low in the group printed at 30°. Beside a print angle, layer thickens also impact on the characteristics of 3D printing product (Alghauli et al., 2025), a layer thickness of 50 μm using an LCD at a time showed the best marginal fit at 30°group in this study.

Moreover, Ryu et al. (2020) excluded printing angles of 90°, 240°, and 270° from their experiment, with the buccal or lingual surface positioned on the build platform. These angles tilted the prosthesis close to a vertical position, which negatively affected marginal adaptation due to the influence of gravity. Similarly, in the pilot test of the present study, printing angles of 60° and 90° were excluded for the same reason, as they hindered passive adaptation. This may be attributed to internal distortion caused by gravity acting on unsupported areas during the printing process.

All printing angles in this study showed marginal gaps within the clinically acceptable threshold of 120 μm (Ryu et al., 2020), indicating that the prostheses produced at each angle met the criteria for functional adaptation.

The surface roughness (Ra and Rz) showed statistically significant differences depending on the printing angle. Both values were lowest at 0° group, followed by 45°, 30°, and 15° groups in that order. In this study, stair-stepping patterns formed by the layer-by-layer additive manufacturing process were observed in the 45°, 30°, and 15° groups, with the widest spacing observed in the 15° group. This pattern was not present in the 0° group, where the layers, oriented horizontally, were stacked vertically. Such surface features may have contributed to the highest surface roughness observed at 15°.

However, it should be noted that surface roughness in this study was measured using flat disc specimens for consistency. Such specimens do not replicate the anatomical complexity of clinical crowns, particularly in the buccal, lingual, mesial, and distal areas where plaque and calculus tend to accumulate. In addition, the printing angle in this study was applied based on the occlusal surface. When printed at 0°, the lateral surfaces of the crown may be positioned at much steeper angles, sometimes nearly vertical. Therefore, it is difficult to fully generalize these findings to all clinically relevant surfaces.

Alharbi and Osman (2021) compared the surface roughness of the labial surface of specimens printed using a maxillary anterior tooth according to the printing angle. They reported that at 0°, where the incisal edge faced the build platform, the stair-step spacing on the labial surface was relatively narrow, and the surface roughness was the lowest. In the present study, with the exception of the 0° group, increasing the printing angle resulted in narrower stair-step spacing and reduced surface roughness. Combining the findings of both studies, the nearly vertical lateral surfaces of a maxillary molar may exhibit the lowest surface roughness when printed at 0°. These findings provide

useful insights, although their study used an SLA printer, and the applicability to LCD-printed FDPs remains unclear due to fundamental differences in printer structure and curing mechanisms.

Pilot tests of this study revealed inaccuracies in the printed crowns positioned at the edge of the build platform. Most photopolymerization 3D printers utilize a rear supported build platform that moves vertically. During vertical movement, vibrations are more likely to occur at the unsupported edges than at the centrally fixed area, leading to dimensional deviations (Unkovskiy et al., 2018). In addition, the peel force generated during the separation of each cured layer from the resin tank may further amplify these vibrations. Therefore, to minimize errors caused by the mechanical or operational aspects, all test specimens were printed at the center of the build platform.

LCD-based systems have structural limitations. According to Shafique et al. (2024), the use of crossed polarizers in LCD panels significantly reduces transmittance, lowering the irradiance reaching the resin surface to approximately 2–3 mW/cm². This is much lower than the 5–100 mW/cm² typically observed in DLP systems. They reported that such low irradiance may limit the rate of polymerization, especially when printing large volumes or high-resolution objects. However, the LCD printer used in this study (Anycubic Photon Mono M7 Pro) is equipped with a COB LED light source system, Fresnel lenses, and a front-facing reflector. It provides an irradiance of 5.5 mW/cm² and over 90% light uniformity, which compensates for the above-mentioned limitations.

This study has several limitations:

First, only one LCD 3D printer and one type of resin were used, so the results cannot be generalized to all LCD 3D printers and 3D printing resins.

Second, a cobalt-chromium model, which has a higher elastic modulus than natural teeth, was used as the master model. Previous studies have reported that models with a higher elastic modulus

show higher fracture loads. Therefore, the use of a cobalt-chromium model may have influenced the high fracture load values observed in this study (Reymus et al., 2020).

Third, surface roughness was evaluated using circular disc specimens instead of crown-shaped specimens. The measurement did not include the lateral surfaces. Therefore, it may be difficult to generalize the results to all clinical situations.

Lastly, this study was conducted in vitro and did not reproduce intraoral conditions. According to previous studies, reproducing the oral environment during experiments, such as thermal cycling and the presence of saliva, can significantly affect provisional materials (Diken Turksayar et al., 2022; Doh et al., 2025). Therefore, different results may be obtained if experiments are conducted under conditions that simulate the oral environment.

Considering these limitations, future studies may consider using a wider variety of 3D printers and materials. In addition, the use of specimens and master models that closely resemble natural teeth, along with experiments conducted under conditions similar to the oral environment, could enhance clinical relevance. Finally, further research may be needed to investigate the influence of printing position on the accuracy of LCD printers.

5. CONCLUSION

This study demonstrated that the printing angle influences the properties of 3D printed objects fabricated using an LCD printer. Significant differences were observed in fracture strength, marginal adaptation, and surface roughness across the tested angle groups (0°, 15°, 30°, and 45°), suggesting that printing orientation could be a critical factor when optimizing the clinical performance of provisional FDPs.

1. The fracture strengths of 0° and 15° printing angle groups were higher than those of the 30° and 45° groups. The provisional prostheses printed at each angle group exceeded the average maximum occlusal force.

2. The smallest marginal gap was in the 30° group, with the lowest mean and standard deviation. All groups showed clinically acceptable values of marginal gap below 120 μm.

3. Surface roughness increased in the order of 0°, 45°, 30°, and 15°. Except for the 0° group, increasing the printing angle resulted in narrower stair-step spacing and reduced surface roughness.

No single angle was superior in all aspects tested. Based on the results of this study, the printing angles of 0° and 30° may be considered favorable options.

REFERENCES

Alghauli, M. A., Aljohani, R., Almuzaini, S., Aljohani, W., Almutairi, S., & Alqutaibi, A. Y. (2025). Accuracy, Marginal, and Internal Fit of Additively Manufactured Provisional Restorations and Prostheses Printed at Different Orientations. *Journal of Esthetic and Restorative Dentistry*, *37*(4), 934-949.

Alharbi, N., Osman, R., & Wismeijer, D. (2016). Effects of build direction on the mechanical properties of 3D-printed complete coverage interim dental restorations. *Journal of Prosthetic Dentistry*, *115*(6), 760-767.

Alharbi, N., & Osman, R. B. (2021). Does build angle have an influence on surface roughness of anterior 3D-printed restorations? An in-vitro study. *International Journal of Prosthodontics*, *34*(4), 505-510.

Caussin, E., Moussally, C., Le Goff, S., Fasham, T., Troizier-Cheyne, M., Tapie, L., Dursun, E., Attal, J. P., & François, P. (2024). Vat Photopolymerization 3D Printing in Dentistry: A Comprehensive Review of Actual Popular Technologies. *Materials*, *17*(4), 950.

Chen, H., Cheng, D.-H., Huang, S.-C., & Lin, Y.-M. (2021). Comparison of flexural properties and cytotoxicity of interim materials printed from mono-LCD and DLP 3D printers. *Journal of Prosthetic Dentistry*, *126*(5), 703-708.

Cho, S.-M., Oh, K. C., Park, J.-M., Lim, J.-H., & Kwon, J.-S. (2023). Comparative assessment of marginal and internal gaps of cast-free monolithic zirconia crowns fabricated from 2 intraoral scanners: A prospective, double-blind, randomized clinical trial. *Journal of Prosthetic Dentistry*, *129*(1), 69-75.

Diken Turksayar, A. A., Donmez, M. B., Olcay, E. O., Demirel, M., & Demir, E. (2022). Effect of printing orientation on the fracture strength of additively manufactured 3-unit interim fixed dental prostheses after aging. *Journal of Dentistry*, *124*, 104155.

Doh, R. M., Choi, W. I., Kim, S. Y., & Jung, B. Y. (2025). Mechanical properties of a polylactic 3D-printed interim crown after thermocycling. *PLoS One*, *20*(1), e0318217.

Fábio Hideo, K., Eliane Cristina Gava, P., Fabiana Gouveia, S., Galvani, L. D., Kuga, M. C., Thalita Ayres, A., Ageu Raupp, J., Marcus Vinícius Reis, S., Jefferson Ricardo, P., & Vidotti, H.

(2025). Influence of Printing Orientation on the Mechanical Properties of Provisional Polymeric Materials Produced by 3D Printing. *Polymers*, *17*(3), 265.

Grymak, A., Aarts, J. M., Ma, S., Waddell, J. N., & Choi, J. J. E. (2021). Comparison of hardness and polishability of various occlusal splint materials. *Journal of the Mechanical Behavior of Biomedical Materials*, *115*, 104270.

Hasanzade, M., Zabandan, D., Mosaddad, S. A., & Habibzadeh, S. (2023). Comparison of marginal and internal adaptation of provisional polymethyl methacrylate restorations fabricated by two three-dimensional printers:An in vitro study. *Dental Research Journal*, *20*(1), 87.

Kessler, A., Reymus, M., Hickel, R., & Kunzelmann, K.-H. (2019). Three-body wear of 3D printed temporary materials. *Dental Materials*, *35*(12), 1805-1812.

Lin, C.-H., Lin, Y.-M., Lai, Y.-L., & Lee, S.-Y. (2020). Mechanical properties, accuracy, and cytotoxicity of UV-polymerized 3D printing resins composed of Bis-EMA, UDMA, and TEGDMA. *Journal of Prosthetic Dentistry*, *123*(2), 349-354.

Murat, S., Alp, G., Alatalı, C., & Uzun, M. (2019). In Vitro Evaluation of Adhesion of Candida albicans on CAD/CAM PMMA-Based Polymers. *Journal of Prosthodontics*, *28*(2), e873-e879.

Park, G.-S., Seong-Kyun, K., Seong-Joo, H., Jai-Young, K., & Seo, D.-G. (2019). Effects of Printing Parameters on the Fit of Implant-Supported 3D Printing Resin Prosthetics. *Materials*, *12*(16), 2533.

Reeponmaha, T., Angwaravong, O., & Angwarawong, T. (2020). Comparison of fracture strength after thermo-mechanical aging between provisional crowns made with CAD/CAM and conventional method. *Journal of Advanced Prosthodontics*, *12*(4), 218-224.

Reymus, M., Fabritius, R., Kessler, A., Hickel, R., Edelhoff, D., & Stawarczyk, B. (2020). Fracture load of 3D-printed fixed dental prostheses compared with milled and conventionally fabricated ones: the impact of resin material, build direction, post-curing, and artificial aging-an in vitro study. *Clinical Oral Investigations*, *24*(2), 701-710.

Rosentritt, M., Huber, C., Strasser, T., & Schmid, A. (2021). Investigating the mechanical and optical properties of novel Urethandimethacrylate (UDMA) and Urethanmethacrylate (UMA) based rapid prototyping materials. *Dental Materials*, *37*(10), 1584-1591.

Ryu, J. E., Kim, Y. L., Kong, H. J., Chang, H. S., & Jung, J. H. (2020). Marginal and internal fit of

3D printed provisional crowns according to build directions. *Journal of Advanced Prosthodontics*, *12*(4), 225-232.

Sang-Mo, P., Ji-Man, P., Seong-Kyun, K., Seong-Joo, H., & Jai-Young, K. (2019). Comparison of Flexural Strength of Three-Dimensional Printed Three-Unit Provisional Fixed Dental Prostheses according to Build Directions. *Journal of Korean Dental Science*, *12*(1), 13-19.

Shafique, H., Karamzadeh, V., Kim, G., Shen, M. L., Morocz, Y., Sohrabi-Kashani, A., & Juncker, D. (2024). High-resolution low-cost LCD 3D printing for microfluidics and organ-on-a-chip devices. *Lab on a Chip*, *24*(10), 2774-2790.

Son, K., Lee, S., Kang, S. H., Park, J., Lee, K. B., Jeon, M., & Yun, B. J. (2019). A Comparison Study of Marginal and Internal Fit Assessment Methods for Fixed Dental Prostheses. *Journal of Clinical Medicine*, *8*(6), 785.

Tsolakis, I. A., Gizani, S., Panayi, N., Antonopoulos, G., & Tsolakis, A. I. (2022). Three-Dimensional Printing Technology in Orthodontics for Dental Models: A Systematic Review. *Children*, *9*(8), 1106.

Unkovskiy, A., Bui, P. H., Schille, C., Geis-Gerstorfer, J., Huettig, F., & Spintzyk, S. (2018). Objects build orientation, positioning, and curing influence dimensional accuracy and flexural properties of stereolithographically printed resin. *Dental Materials*, *34*(12), e324-e333.

Wada, J., Wada, K., Gibreel, M., Wakabayashi, N., Iwamoto, T., Vallittu, P. K., & Lassila, L. (2022). Effect of 3D Printer Type and Use of Protection Gas during Post-Curing on Some Physical Properties of Soft Occlusal Splint Material. *Polymers*, *14*(21), 4618.

Yang, J., Liang, X., Liu, F., Biao, Y., & He, J. (2024). Comparing Properties of Urethane Dimethacrylate (UDMA) Based 3D Printing Resin Using N-Acryloylmorpholine (ACMO) and Triethylene Glycol Dimethacrylate (TEGDMA) Separately as Diluents. *Journal of Macromolecular Science, Part B: Physics*.

Yildirim, M., Aykent, F., & Ozdogan, M. S. (2024). Comparison of fracture strength, surface hardness, and color stain of conventionally fabricated, 3D printed, and CAD-CAM milled interim prosthodontic materials after thermocycling. *Journal of Advanced Prosthodontics*, *16*(2), 115-125.

ABSTRACT IN KOREAN

3D 프린팅 출력 각도에 따른 임시 치관의 기계적 물성, 마진 적합도 및 표면 거칠기의 비교

치과의 전반적인 과정이 디지털 워크플로우로 진행됨에 따라 3D 프린팅을 이용한 임시 보철물 제작이 이루어지고 있다. 특히, 3D 프린터 중 액정 디스플레이(liquid crystal display, LCD) 방식의 3D 프린터는 저렴한 가격과 임상적으로 허용가능한 성능으로 인해 쉽게 보급되고 있다. 그러나 3D 프린팅은 출력 각도에 따라 출력 결과의 기계적 및 표면 특성에 상당한 영향을 미칠 수 있다. 본 연구의 목적은 LCD 3D 프린터를 사용하여 제작된 단일 임시 크라운의 파절 강도, 마진 적합도 그리고 표면 거칠기에 미치는 다양한 출력 각도의 영향을 평가하는 것이다.

마스터 모형은 팬텀 치아를 임상적 기반으로 prep 한 후 코발트-크롬으로 복제되었다. 시험에 사용된 시편은 임시 크라운과 디스크 두가지 형태로 설계되었다. 각 시편은 우레탄 디메타크릴레이트(urethane dimethacrylate, UDMA) 기반 3D 프린팅 레진을 사용하여 0°, 15°, 30°, 45°의 네 가지 다른 출력 각도로 프린팅 되었다. 각 시험 마다 4 가지 각도로 19 개씩, 총 76 개의 시편을 제작했다.

파괴 시험에는 만능재료시험기를 사용했다. 하중을 가하는 동안 크로스헤드는 1 mm/min 의 속도로 이동하도록 설정하였다. 마진 적합도는 실리콘 복제 기술(silicone replica technique, SRT)을 통해 평가되었으며, 협측, 근심측, 원심측 및 설측 표면에서 측정되었다. 표면 거칠기는 공초점 레이저 주사 현미경을 사용하여 디스크의 9 개 지점을 측정하였다. 이 측정값들은 평균을 내어 한 개의 시편 결과값을 얻고, 각도별로 시편의 평균과 표준편차를 내어 비교하였다. Shapiro-Wilk 검정은 정규성을

평가하는 데 사용되었다. 정규성이 충족되면 일원 분산 분석(one-way ANOVA)을 적용했다. 이 가정이 어긋나는 경우에는 Kruskal-Wallis 검정을 대신 수행하였다. 개별 집단 간의 차이를 평가하기 위해 1 차 검정 후 Bonferroni 사후 비교를 수행하였다.

분석 결과는 세 가지 시험 항목 모두에서 출력 각도에 따른 통계적으로 유의미한 차이를 나타냈다($p < 0.05$). 0° 및 15° 로 인쇄된 군이 30° 및 45°로 인쇄된 군보다 더 높은 파절 강도를 보였으며, 모든 각도에서 평균 최대 교합력을 초과했다. 마진 간극은 30° 그룹에서 가장 작은 평균 및 표준편차로 나타났으며, 모든 각도에서 임상적 허용 값인 120 μm 미만을 충족하였다. 표면 거칠기는 0°, 45°, 30°, 15° 순서로 증가했다. 0° 그룹을 제외하고 인쇄 각도가 증가할수록 층간 간격이 좁아지고 표면 거칠기가 감소했다.

본 연구의 결론은 LCD 프린터를 사용하여 제작된 출력물의 특성에 인쇄 각도가 영향을 미친다는 것이다. 그러나 모든 측면에서 단일 각도가 우월성을 보인 것은 아니다. 따라서 특정 임상 상황에 따라 인쇄 각도를 선택해야 한다. 본 연구를 바탕으로 0°와 30° 인쇄 각도 사용을 추천할 수 있다.

핵심 되는 말 : 3D 프린터, LCD 3D 프린터, 출력 각도, 파절 강도, 마진 적합도, 실리콘 복제 기법(SRT), 표면 거칠기